THE REACTION POMERON–POMERON $\rightarrow \pi^+\pi^-$ AND AN UNUSUAL PRODUCTION MECHANISM FOR THE $f_2(1270)$

Ames–Bologna–CERN–Dortmund–Heidelberg–Warsaw Collaboration

A. Breakstone[1*], R. Campanini[2], H.B. Crawley[1], G.M. Dallavalle[2], M.M. Deninno[2], K. Doroba[6], D. Drijard[3], F. Fabbri[3], A. Firestone[1], H.G. Fischer[3], H. Frehse[3**], W. Geist[3***], G. Giacomelli[2], R. Gokieli[6], M. Gorbics[1†], P. Hanke[5], M. Heiden[3††], W. Herr[5†††], L.D. Isenhower[1°], E.E. Kluge[5], J.W. Lamsa[1], R.A. Leacock[1], T. Lohse[4††††], R. Mankel[4], W.T. Meyer[1], G. Mornacchi[3], T. Nakada[5°°], M. Panter[3°°°], A. Putzer[5], K. Rauschnabel[4], B. Rensch[5], F. Rimondi[2], M. Schmelling[4‡], G.P. Siroli[2], J.D. Skeens[1‡‡], R. Sosnowski[6], M. Szczekowski[6], O. Ullaland[3], D. Wegener[4], and R. Yeung[3‡‡‡]

1 Ames Laboratory and Physics Department, Iowa State Univ., Ames, USA
2 Istituto di Fisica dell'Universita and INFN, Bologna, Italy
3 CERN, European Organization for Nuclear Research, Geneva, Switzerland
4 Institut für Physik der Universität, Dortmund, Germany
5 Institut für Hochenergiephysik, Heidelberg, Germany
6 University and Institute for Nuclear Research, Warsaw, Poland

Submitted to Zeitschrift für Physik C

---

* Present address: University of Hawaii, USA
** Present address: CONVEX, Zürich, Switzerland
*** Present address: CRN Strasbourg, France
† Present address: LeCroy Research Systems, Chestnut Ridge, NY, USA
†† Present address: DEC, Kaufbeuren, Germany
††† Present address: CERN, Geneva, Switzerland
° Present address: Abilene Christian University, Texas, USA
°° Present address: Paul Scherer Institute, Villigen, Switzerland
°°° Present address: Max Planck Institute, Heidelberg, Germany
‡ Present address: University of Mainz, Germany
‡‡ Present address: Rice University, Houston, Texas, USA
‡‡‡ Present address: CALTECH, Pasadena, California, USA

ABSTRACT

Data are presented on Pomeron-Pomeron interactions which produce a central $\pi^+\pi^-$ system in proton-proton collisions at $\sqrt{s} = 62$ GeV at the CERN ISR. This process may favor the production of gluonic bound states. A partial-wave analysis of the $\pi^+\pi^-$ system shows evidence for the production of the states $f_0(975)$, $f_0(1400)$, and $f_2(1270)$. The fitted mass for the $f_2(1270)$ is about 50 MeV below the world average. In addition, the production mechanism for the $f_2(1270)$ is uniquely different from that for the other final states in that there is a correlation between the outgoing protons. This is consistent with a picture of two-gluon exchange with the $f_2(1270)$ produced by gluon fusion, and could indicate that the $f_2(1270)$ has a glueball component.

1. Introduction

It is a prediction of QCD that there exist hadrons, called glueballs, which are built up by valence gluons. They are expected to have masses in the region less than about 2 GeV. Glueballs may not be easily produced in normal peripheral reactions which are presumably dominated by quark processes, but are expected to be generated in processes having high gluonic content, like Double-Pomeron-Exchange (DPE) [1]. The Pomeron, **P**, is assumed to be a multi-gluon state with the quantum numbers of the vacuum [2]. We note that, glueballs, even if produced, may be difficult to identify due to their possible mixture with $q\bar{q}$ states.

In this paper, we present an examination of DPE from the reaction

$$pp \rightarrow pp\pi^+\pi^- \tag{1}$$

at a center-of-mass (c.m.s.) energy $\sqrt{s} = 62$ GeV. Collisions of the type expected for Pomeron-Pomeron interactions are obtained by selecting two diffractively scattered protons at large Feynman-x, x_f, and a centrally produced system. The exchanged Pomerons produce the reaction

$$\mathbf{PP} \rightarrow \pi^+\pi^-, \tag{2}$$

as shown in Fig. 1. Pomeron-Pomeron interactions can produce only $I = 0$ states with $J^{PC} = 0^{++}$, 2^{++}, 4^{++}, etc. Previous studies of reaction (2) can be found in Refs. [3–6].

2. Data Acquisition and Selection

The Intersecting Storage Rings (ISR) at CERN provided good conditions for the study of reaction (1) because of their high luminosity and open geometry; i.e., the experiments

were performed essentially in the c.m.s. of the colliding protons. Data were taken at $\sqrt{s}$ = 62 GeV with the Split-Field-Magnet (SFM) detector [7], which had a 1 Tesla field and very good solid-angle coverage (~95%) for charged particles. It was composed of multiwire proportional chambers (MWPC) arranged into a central detector plus two forward telescopes along the outgoing beams. A system of time-of-flight (TOF) counters for particle identification surrounded the central detector.

The trigger required a fast charged particle in each forward telescope, plus at least one charged particle detected in the central region. Included was a veto on charged particles produced at intermediate polar angles; this imposed a rapidity gap of at least two units between each fast proton and the charged particles produced in the central region. The integrated luminosity was 50 nb^{-1}.

Events satisfying the trigger conditions were processed with the standard SFM reconstruction codes. Events with one positive forward track in each of the two telescopes with $|x_f| > 0.7$ and two central ($|x_f| < 0.3$) tracks of opposite charge were selected. In order to reject events with additional neutral particles and to assign to them the correct hypothesis, the selected events were subjected to a four-constraint kinematic fit. Background from other channels, such as ppK^+K^-, was estimated to be less than 15%. The final data sample consists of 16400 events.

In previous work we published evidence that, in the above trigger configuration, reaction (1) is dominated by Double-Pomeron-Exchange [5,6]. A cross-section of $\simeq$ 80 μb was determined for reaction (1) [6].

3. Acceptance Corrections

Acceptances have been calculated using a two-stage Monte-Carlo technique. In the first stage, single particles were generated for all momenta and angles that could envelop the trigger chambers (including the veto). The particle trajectories were tracked through the magnetic field and the detector chambers [8]. Energy losses, scattering, and particle decays were included. With the information obtained from this tracking, 'trigger-tables' were constructed which define the regions (in polar angle θ, azimuth ϕ, and momentum p) where particle trajectories satisfied one of the trigger requirements.

In the second stage, complete events were generated using a double-peripheral model [9]. Peripheral production of the outgoing protons was simulated by using the matrix-element squared $exp(6\,t_1) \cdot exp(6\,t_2)$, where t_1 and t_2 are the four-momentum-transfers squared from initial to final-state protons. The t distributions produced with this model agree with the data. An isotropic angular distribution was used for the decay of the central

system to $\pi^+\pi^-$. Acceptance tables were calculated for 0.1 GeV intervals of the invariant $\pi^+\pi^-$ mass, $M(\pi^+\pi^-)$, in two dimensions corresponding to the decay angles θ and ϕ, defined with respect to the Pomeron direction in the $\pi^+\pi^-$ system.

The trigger acceptance for a Monte-Carlo event was obtained by examining each track in the event against the 'trigger-tables' to determine if the trigger requirement was satisfied. To obtain the full acceptance, the trigger acceptance was combined with the SFM track reconstruction efficiency calculated for the complete event. The full acceptance, for an isotropic decay, increases smoothly from 0.003 to 0.006 over the $\pi^+\pi^-$ mass range 0.4 to 2.0 GeV. We note that a large fraction of the acceptance correction results from the trigger requirement for the forward protons.

4. Characteristics of the $\pi^+\pi^-$ System

The $\pi^+\pi^-$ invariant mass distribution, corrected for acceptance, is shown in Fig. 2 for the events of reaction (1). The 'starred' points result from the fit, described later. The mass distribution features a wide low-mass enhancement centered at about 0.7 GeV. It falls rapidly near 1.0 GeV and peaks again near 1.250 GeV. There is no evidence for the $\rho(770)$ which is consistent with little background from non-Pomeron exchange.

We have examined the moments of the spherical harmonics, $\langle Y_m^l(cos\theta,\phi)\rangle$, of the corrected $\pi^+\pi^-$ decay angular distribution. The polar decay angle θ is defined by the π^+ direction with respect to the incident exchange particles in the $\pi^+\pi^-$ rest system. The azimuthal angle ϕ is the angle between the $\pi^+\pi^-$ decay plane and the PP production plane in the total c.m.s.. Moments up to $l=6$ were examined. No evidence for contributions from magnetic substates other than $m=0$ was found, which is consistent with DPE. Also, for $M(\pi^+\pi^-) < 2.0$ GeV, spins less than $J=4$ are sufficient to describe the moments. We therefore assume, for PP interactions, that the only contributions to our data are from $J=0,2$ $(m=0)$, i.e., from S and D-wave.

We have parametrized the angular distribution in terms of density-matrix elements $\rho^{J_1 J_2}$, in a manner similar to Ref.[4]:

$$A(cos\theta) = (N/2)\ \{\ \rho^{SS} + 2\sqrt{4\pi}\ \rho^{SD}\ Y_0^2(cos\theta) + 4\pi\ \rho^{DD}\ [Y_0^2(cos\theta)]^2\ \}, \qquad (3)$$

where

$$0 \le \rho^{SS} \le 1, \qquad \rho^{SS} + \rho^{DD} = 1, \qquad |\rho^{SD}|^2 \le |\rho^{SS}||\rho^{DD}| \qquad (4)$$

and N is the number of events in a given mass interval.

A least-squares fit for the two independent variables ρ^{SS} and ρ^{SD} was performed to the acceptance corrected angular distributions as a function of $M(\pi^+\pi^-)$. The resulting

values for ρ^{SS} and ρ^{SD} are shown in Figs. 3 and 4 for $M(\pi^+\pi^-) \leq 2.25$ GeV. It can be seen that the data are strongly dominated by the S-wave below 1.0 GeV.

The S and D-wave contributions are given by:

$$|S|^2 = N\rho^{SS}, \qquad |D|^2 = N\rho^{DD}, \tag{5}$$

and $\rho^{SD} = Re\, S^* D/(|S|^2 + |D|^2)$. The cross-sections for S and D-wave, with acceptance correction, are shown in Figs. 5 and 6. In addition to the low-mass (S-wave) enhancement, there are enhancements in both the S and D-wave cross-sections centered around $M(\pi^+\pi^-) = 1.250$ GeV, near the mass of the $f_2(1270)$ and $f_0(1400)$. The S-wave cross-section falls rapidly near 1.0 GeV, close to the $f_0(975)$ mass.

To determine the resonance contributions in our data, we have performed a simultaneous fit to the mass dependence of $|S|^2$, $|D|^2$, and ρ^{SD}. To best describe the low-mass S-wave enhancement, we have chosen the following background amplitude, $BG = A/\left[(M_{\pi\pi} - M_0)^n + B\right]^{1/2}$ with adjustable parameters A, B, M_0, and n ($n \simeq 3$ from the fit). This term was taken in product with contributions from resonant S-wave Breit-Wigner amplitudes. To account for the continuum D-wave cross-section at higher masses we similarly included a background term of the same form as for the S-wave, but with different values for the parameters. This term was multiplied by a D-wave Breit-Wigner amplitude. Breit-Wigner (S-wave) functions were included for the $f_0(975)$ and $f_0(1400)$ states, and a D-wave Breit-Wigner for the $f_2(1270)$ state. The amplitudes were added coherently with relative phases; and, the relative contribution, mass, width and phase of each Breit-Wigner function was fitted [10].

These resonant states together with the background terms gave a good fit to the data, as shown by the 'starred' points in Figs. 2 through 7. The fitted masses and widths for the S-wave states $f_0(975)$ and $f_0(1400)$, given in Table 1, are consistent with previous measurements [11]. We note that the errors on the width and cross-section of the $f_0(1400)$ are quite large; this is due to a strong interference with the S-wave background. To determine if the $M(\pi^+\pi^-)$ bin size, 50 MeV, affects the fitted mass and width of the $f_0(975)$, we repeated the fit with a 25 MeV bin size (equal to the mass resolution near 1.0 GeV). The resulting fitted values were essentially the same. A display of the latter fit for the S-wave is shown in Fig. 7. Production of the $f_0(975)$ has previously been studied in terms of amplitudes and poles [12], and also in terms of the Flatté formalism [13].

For the $f_2(1270)$ we obtained a width of 0.325 ± 0.055 GeV from the fit. Because of the rather large error, we fixed the width for the final fit to 0.200 GeV, a value somewhat larger than the world average. The mass resolution in this region is 35 MeV. In both cases we obtained 1.220 ± 0.010 GeV for the fitted mass of the $f_2(1270)$. This value is about 50

MeV lower than the world average [11]. The correctness of the mass scale has been verified to be better than 10 MeV [5]. The low value for the fitted mass of the $f_2(1270)$ may result uniquely from its production in PP interactions. Along these lines, J.F. Donoghue has calculated such effects from an f-glueball mixture [14]. The fitted values for the mass, width, and cross-section of the $f_0(975)$, $f_0(1400)$, and $f_2(1270)$ are given in Table 1.

5. Production of the $f_2(1270)$ and Factorization

In this section, we study the production mechanism as it relates to the question of factorization at the Pomeron vertices. DPE (Fig.1) predicts an absence of correlation between the two outgoing protons, except for that from kinematics and the trigger acceptance. To examine this question, we calculate the pp azimuthal angle ($\Delta\phi$) between the two outgoing protons in the transverse-momentum plane in the c.m.s., and determine the ratio R:

$$R = (N_G - N_L)/(N_G + N_L), \tag{6}$$

as a function of $M(\pi^+\pi^-)$, where N_G (N_L) is the number of events with $\Delta\phi$ greater (less) than 90°. This is done for the uncorrected data, and for the predictions of the DPE model (including experimental acceptance), see section 3. The results are shown in Fig. 8. The model (solid line) agrees with the data except for the mass region of the $f_2(1270)/f_0(1400)$. The data in this region have a 'back-to-back' correlation ($\Delta\phi > 90°$) between the outgoing protons which is not predicted by the model *.

A partial-wave-analysis was performed independently for two samples of events, one with $\Delta\phi > 90°$, the other with $\Delta\phi < 90°$. Acceptance corrections were also applied for these two cases. The resulting cross-sections for $J = 0, 2$ are shown as a function $M(\pi^+\pi^-)$ in Figs. 9 and 10. The D-wave cross-section near the $f_2(1270)$ for $\Delta\phi > 90°$ exceeds the one for $\Delta\phi < 90°$ by a factor greater than two. For the S-wave in this region there is only a 10−15% difference. We conclude that the proton-proton correlation, in the mass region of the $f_2(1270)/f_0(1400)$, is mainly in the D-wave and is therefore caused by the $f_2(1270)$ production mechanism.

To test whether the $f_2(1270)$ is produced by $f_2/\mathbf{P}$ exchange (as this could produce a proton-proton correlation), we have measured the average absolute value of Feynman-x for the $\pi^+\pi^-$ system, $\langle|x_f(\pi^+\pi^-)|\rangle$, as a function of $M(\pi^+\pi^-)$ for the uncorrected data. Compared to DPE, a model of $f_2/\mathbf{P}$ exchange predicts much larger values of $|x_f(\pi^+\pi^-)|$ (i.e., a flatter $x_f(\pi^+\pi^-)$ distribution), which results because of the different intercepts for

* This may explain why a larger cross-section for $f_2(1270)$ production is measured here than that in Ref.[4], where a more selective trigger rejected the 'back-to-back' configuration.

the f_2 and Pomeron Regge-trajectories (see Ref.[6]). If there were a significant contribution from $f_2/\mathbf{P}$ exchange , an increase (enhancement) in the value of $\langle|x_f(\pi^+\pi^-)|\rangle$ would occur in the mass region of the $f_2(1270)$. The data, however, exhibit a completely smooth behavior through the $f_2(1270)$ region, and we conclude therefore that any contribution from $f_2/\mathbf{P}$ exchange is small.

A more complex model of DPE might break the factorization of the Pomeron vertices. An example of this would be if the central system were formed from the fusion of two gluons (one from each Pomeron), as shown in Fig. 11. Since the remaining gluon[s] are exchanged directly between the two protons, they would induce a correlation between them. Fusion of two gluons might be expected to occur in the mass region of a resonance which has a strong coupling to two gluons. This is consistent with conjectures that the $f_2(1270)$ may contain a glueball mixture [14].

The DPE-model has been modified to simulate the effect of a directly exchanged gluon (Fig. 11). To achieve this an additional final-state elastic scattering of the outgoing protons was included, assuming the form $exp(At)$. The same value of the slope A was used in the matrix-element for the exchanges to produce the central $\pi^+\pi^-$ system. To reproduce the experimental t distributions, $A = 11$ was required. This calculation yields the prediction for the ratio R shown as the dashed line in Fig. 8. The prediction (including experimental acceptance) was found to be insensitive to whether the $\pi^+\pi^-$ system was assumed to be in an S or D-wave. The order of magnitude for the ratio R in the mass region of the $f_2(1270)$ is correctly reproduced (and is corresponding too high for other masses). This model calculation is meant only as a qualitative test to see if the inclusion of a double scattering is able to explain the effect seen for the $f_2(1270)$ mass region. It seems able to.

A glueball nature for the $f_2(1270)$ would be suggested if it were favorably produced by gluon fusion. A detailed calculation from a model with multi-gluon exchange is required before claiming that this is the dominating production mechanism for the $f_2(1270)$, and that it has a glueball mixture.

6. Conclusions

Data have been presented on the production of $\pi^+\pi^-$ systems in the central region from Pomeron-Pomeron reactions in proton-proton collisions at 62 GeV at the CERN ISR. The mass spectrum shows a sudden drop in cross-section near 1.0 GeV, and the $f_2(1270)$ resonance is clearly observed.

Analysis of the angular distributions has shown that the S-wave dominates up to a mass of about 1.0 GeV. The S-wave mass spectrum can be described with a broad low-mass

enhancement plus the scalar meson states $f_0(975)$ and $f_0(1400)$.

The D-wave mass spectrum is described with the $f_2(1270)$ and a broad background. The fitted mass of the $f_2(1270)$ is 1.220 GeV, about 50 MeV lower than the world average. The production mechanism for the $f_2(1270)$ is different from that for the other final states. It is qualitatively consistent with a picture (simple kinematical model) of two-gluon exchange, producing a correlation between the outgoing protons. In this picture, strong production of the $f_2(1270)$ via a gluon-gluon vertex would suggest that it has a glueball mixture.

Acknowledgments

We are grateful for the support provided by the SFM detector group and the ISR Experimental Support group. We wish to thank A. Bialas and P.V. Landshoff for valuable discussions concerning these data. The Dortmund and Heidelberg groups were supported by a grant from the Bundesministerium für Forschung und Technologie of the Federal Republic of Germany. The Ames group was supported by the U.S. Department of Energy under contract W-7405-ENG-82.

References

[1] D. Robson: Nucl. Phys. **B130** (1977) 328

[2] F.E. Low: Phys. Rev. **D12** (1975) 163; S. Nussinov: Phys. Rev. **D14** (1976) 246; J. Pumplin and E. Lehman: Z. Phys. C - Particles and Fields **9** (1981) 25; P.V. Landshoff and O. Nachtmann: Z. Phys. C - Particles and Fields **35** (1987) 405; A. Donnachie and P.V. Landshoff: Nucl. Phys. **B311** (1988/89) 509

[3] R. Waldi, K.R. Schubert, and K. Winter: Z. Phys. C - Particles and Fields **18** (1983) 301; D. Drijard et al.: Nucl. Phys. **B143** (1978) 61; H. DeKerret et al.: Phys. Lett. **68B** (1977) 385; L. Baksay et al.: Phys. Lett. **61B** (1976) 89

[4] T. Åkesson et al.: Nucl. Phys. **133B** (1983) 268; T. Åkesson et al.: Phys. Lett. **B264** (1986) 154

[5] A. Breakstone et al.: Z. Phys. C - Particles and Fields **31** (1986) 185

[6] A. Breakstone et al.: Z. Phys. C - Particles and Fields **42** (1989) 387

[7] R. Bouclier et al.: Nucl. Instr. Meth. **115** (1974) 135; R. Bouclier et al.: Nucl. Instr. Meth. **125** (1975) 19; W. Bell et al.: Nucl. Instr. Meth. **156** (1978) 111

[8] R. Messerli: SFMGENER, CERN (unpublished)

[9] F. James: FOWL, CERN, Program Library (1967); E. Byckling, M. Kaartinen, K. Kajantie, and H. Villanen: Res. Inst. Theor. Phys. Report No. 3-69, 1969 (unpublished)

[10] F. James and M. Roos: MINUIT, CERN, Program Library (1989)

[11] Particle Data Group: Phys. Lett. **204B** (1988) 1

[12] K.L. Au, D. Morgan and M.R. Pennington: Phys. Rev. **D35** (1987) 1633

[13] T.A. Armstrong et al. WA76 Coll.: preprint CERN/EP 88-124 (1988), CERN/EP 89-144 (1989)

[14] J.L. Rosner: Phys. Rev. **D24** (1981) 1347; J.F. Donoghue, K. Johnson and B.A. Li: Phys. Lett. **99B** (1981) 416; J.F. Donoghue: Phys. Rev. **D25** (1982) 1875; S. Minami: preprint OCU-109 (1983)

Table 1. Resonance parameters and cross-sections for exclusive reactions. The quoted errors on cross-sections do not include a systematic error (estimated as a *factor of 1.5*) which results from an overall uncertainty in the acceptance and the luminosity calibration.

Reaction	Mass	Width	Cross Section [μb]
(1) $pp \to pp\,(\pi^+\pi^-)$			79.0 ± 13.0
(2) $pp \to pp\,f_0(975)$	0.956 ± 0.012	0.055 ± 0.015	0.3 ± 0.07
(3) $pp \to pp\,f_0(1400)$	1.275 ± 0.020	0.285 ± 0.060	15.0 ± 4.0
(4) $pp \to pp\,f_2(1270)$	1.220 ± 0.010	$0.200\ (fixed)$	5.0 ± 0.7

Figure Captions

Fig.1 Double-Pomeron-Exchange diagram. A central $\pi^+\pi^-$ system is produced from the collision of two Pomerons (**P**).

Fig.2 Invariant mass distribution for the central $\pi^+\pi^-$, system from reaction (1), in μb per 50 MeV. This and all subsequent figures, show data which have been acceptance corrected, and the 'starred' points represent the result from the fit.

Fig.3 Density-matrix-element ρ^{SS} as a function of $M(\pi^+\pi^-)$.

Fig.4 Density-matrix-element ρ^{SD} as a function of $M(\pi^+\pi^-)$.

Fig.5 Cross-section for S-wave as a function of $M(\pi^+\pi^-)$, in μb per 50 MeV.

Fig.6 Cross-section for D-wave as a function of $M(\pi^+\pi^-)$, in μb per 50 MeV.

Fig.7 Cross-section for S-wave as a function of $M(\pi^+\pi^-)$, in μb per 25 MeV. The result of a fit with this bin size is shown.

Fig.8 Distribution of $R = (N_G - N_L)/(N_G + N_L)$ as a function of $M(\pi^+\pi^-)$. The solid curve shows the prediction of the standard DPE model, the dashed curve is the result of a simulation of two-gluon exchange from a simple kinematical model.

Fig.9 (a) Cross-section for S-wave as a function of $M(\pi^+\pi^-)$, for $\Delta\phi < 90°$. (b) Same as (a) for the D-wave.

Fig.10 (a) Cross-section for S-wave as a function of $M(\pi^+\pi^-)$, for $\Delta\phi > 90°$. (b) Same as (a) for the D-wave.

Fig.11 Double-Pomeron-Exchange diagram with a multi-gluon Pomeron; two gluons fuse to form the central $\pi^+\pi^-$ system, an additional gluon generates a proton-proton correlation.

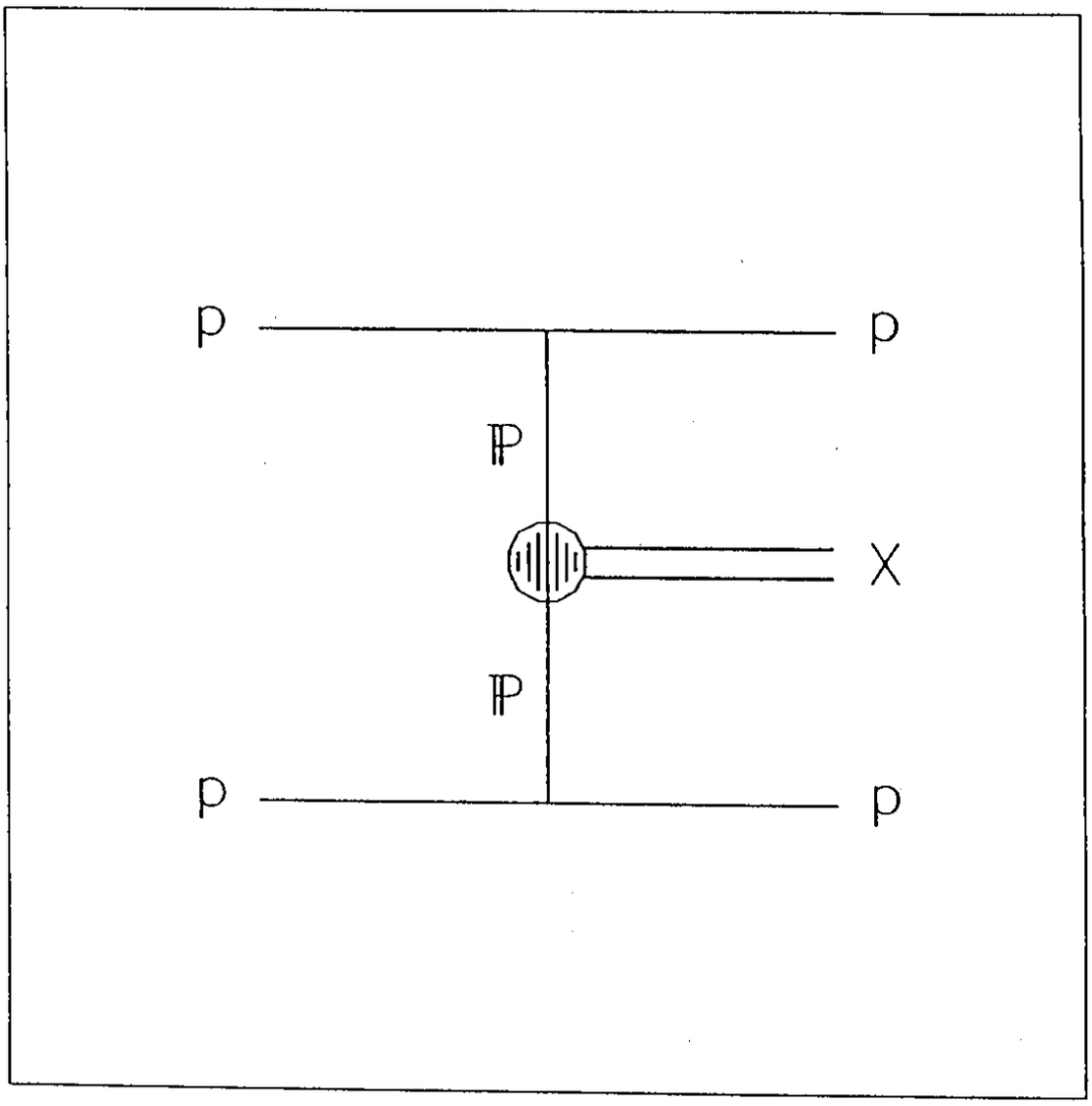

Fig.1

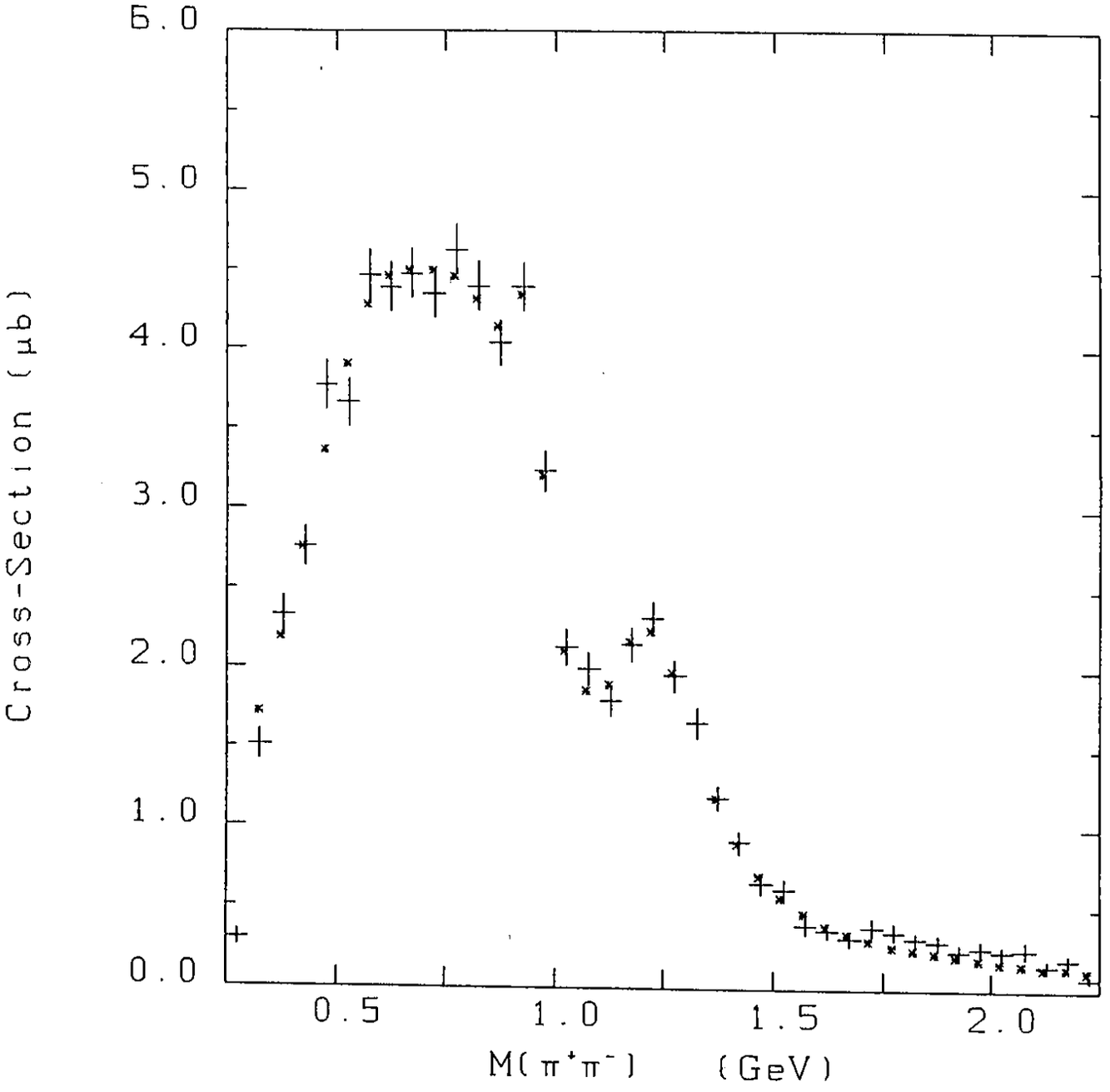

Fig.2

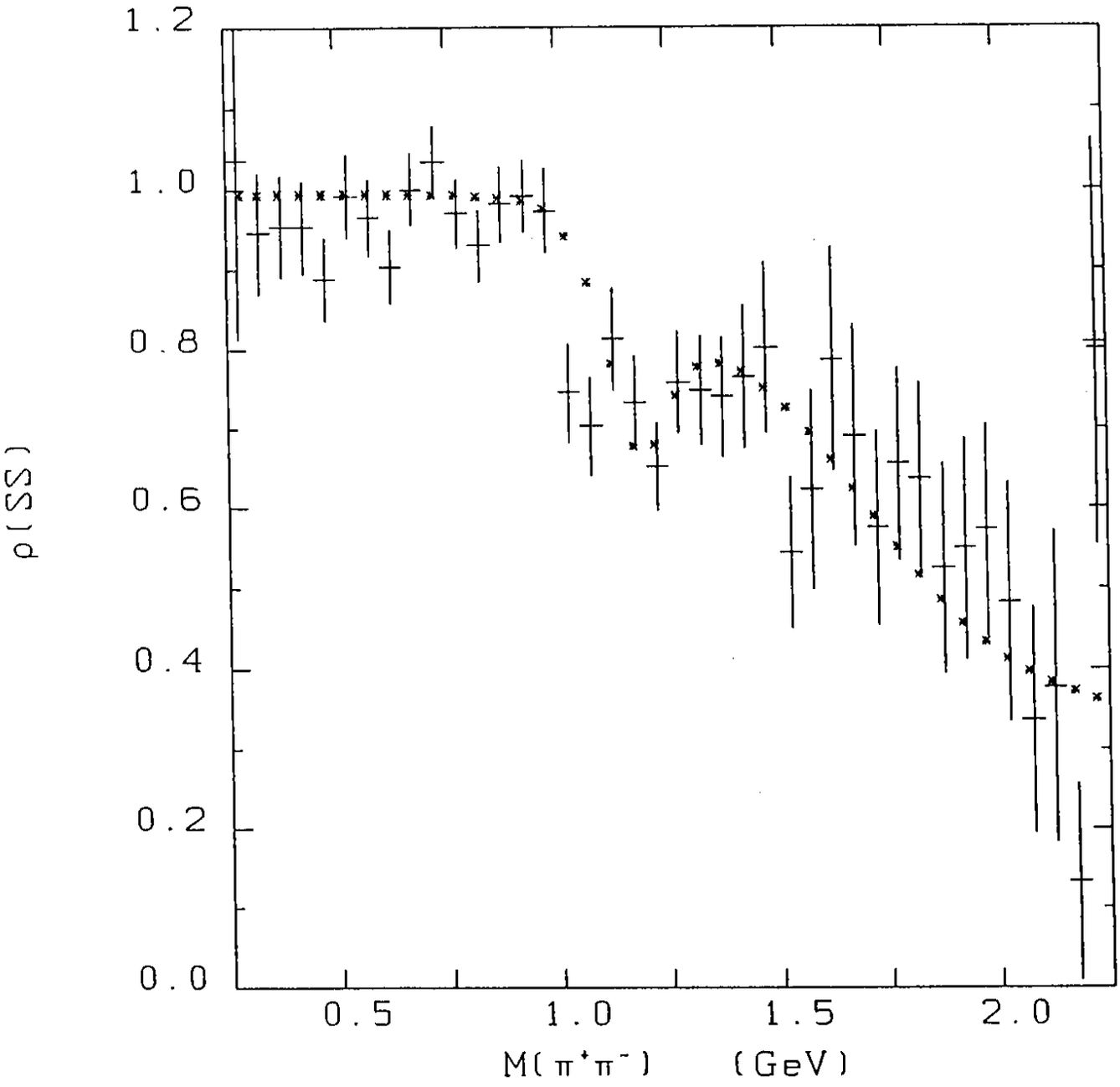

Fig.3

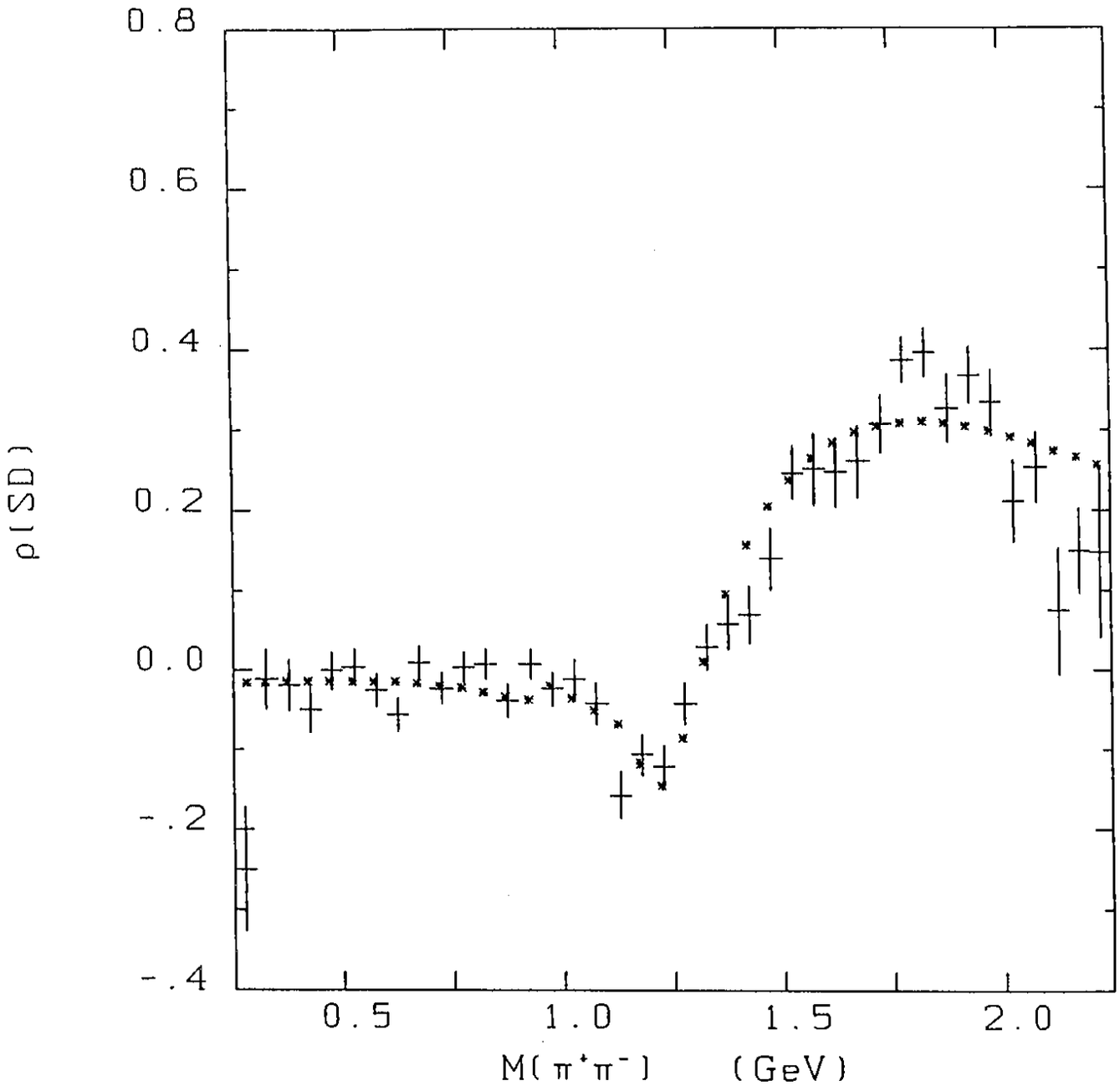

Fig.4

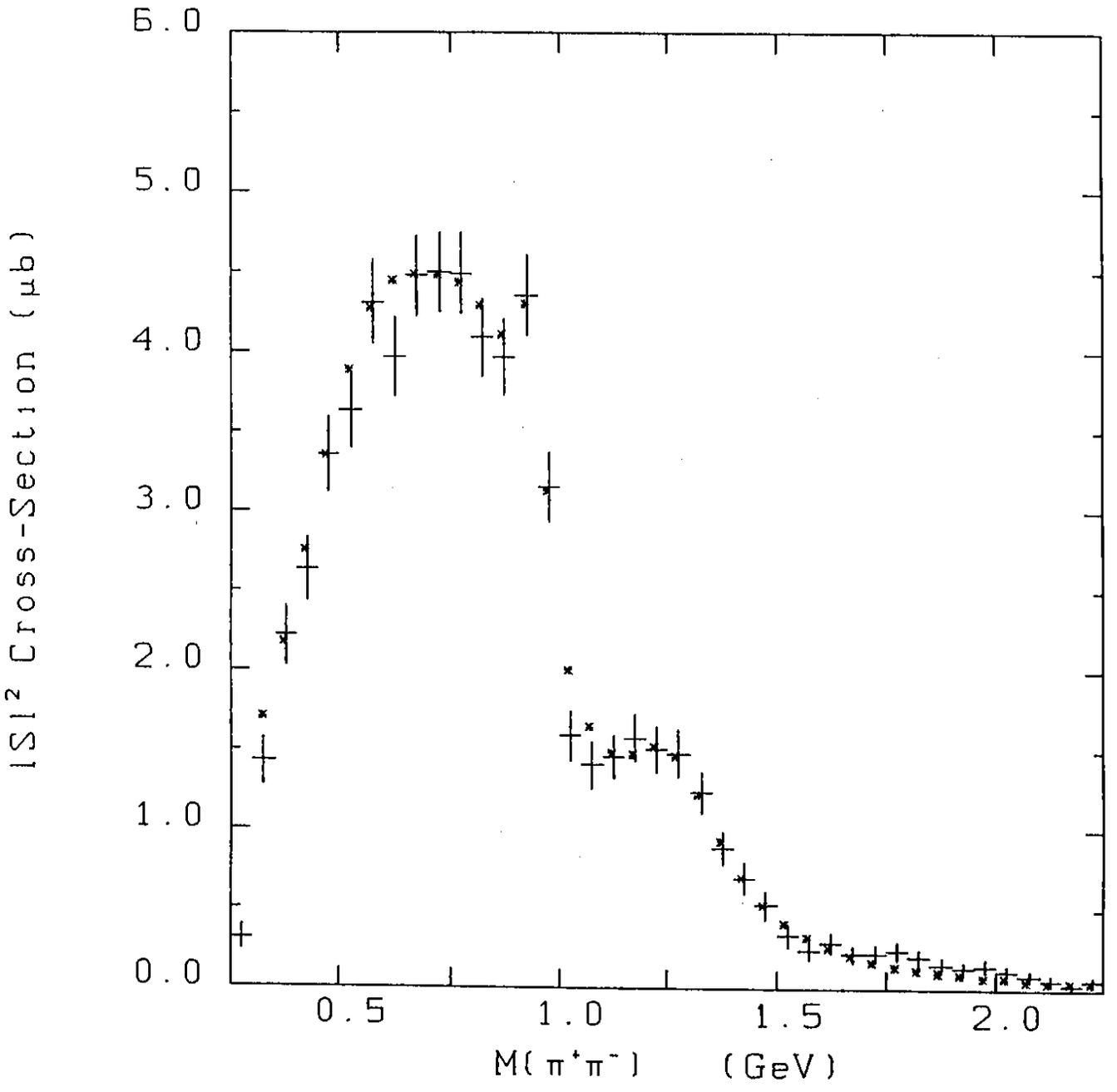

Fig.5

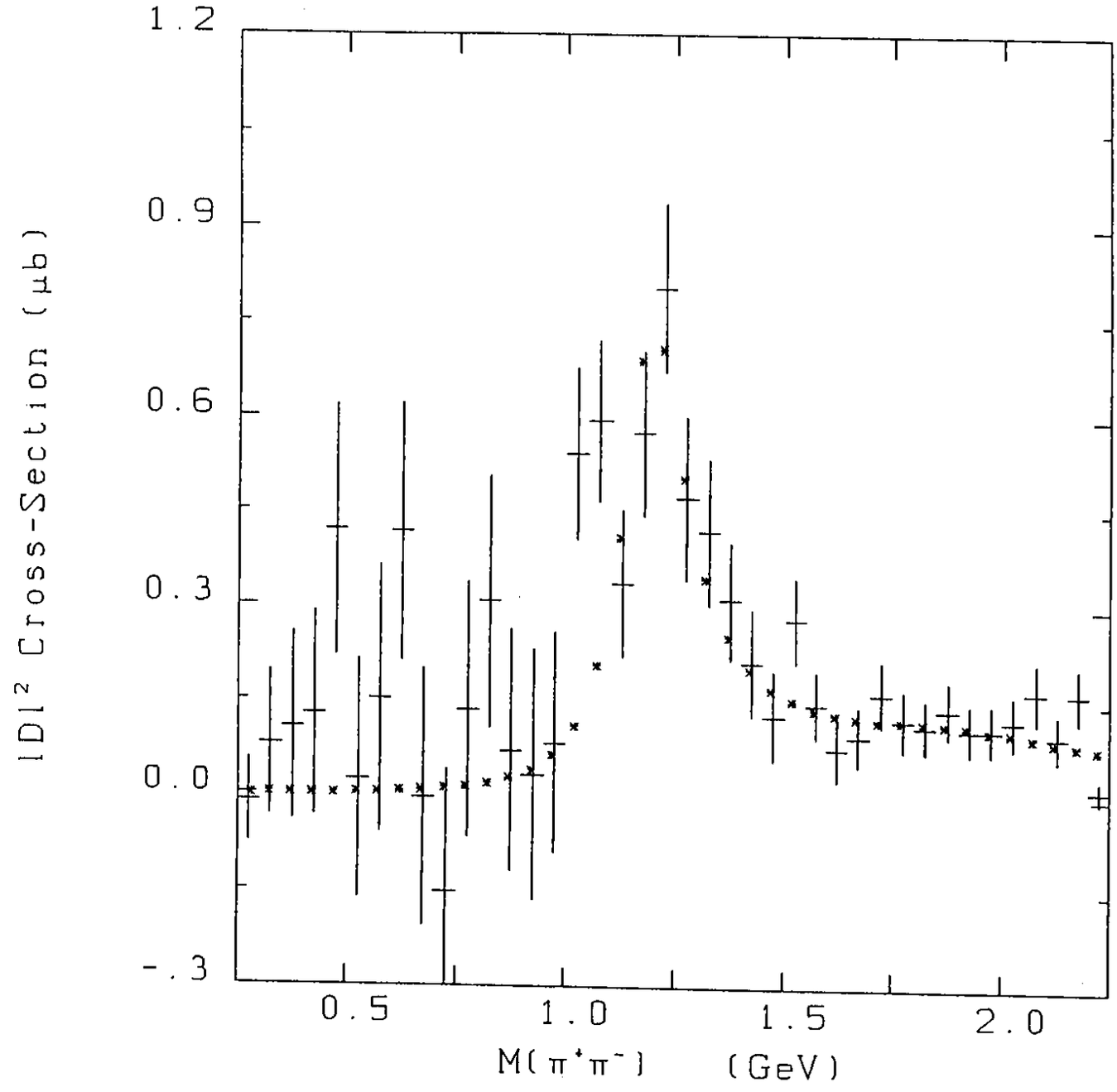

Fig.6

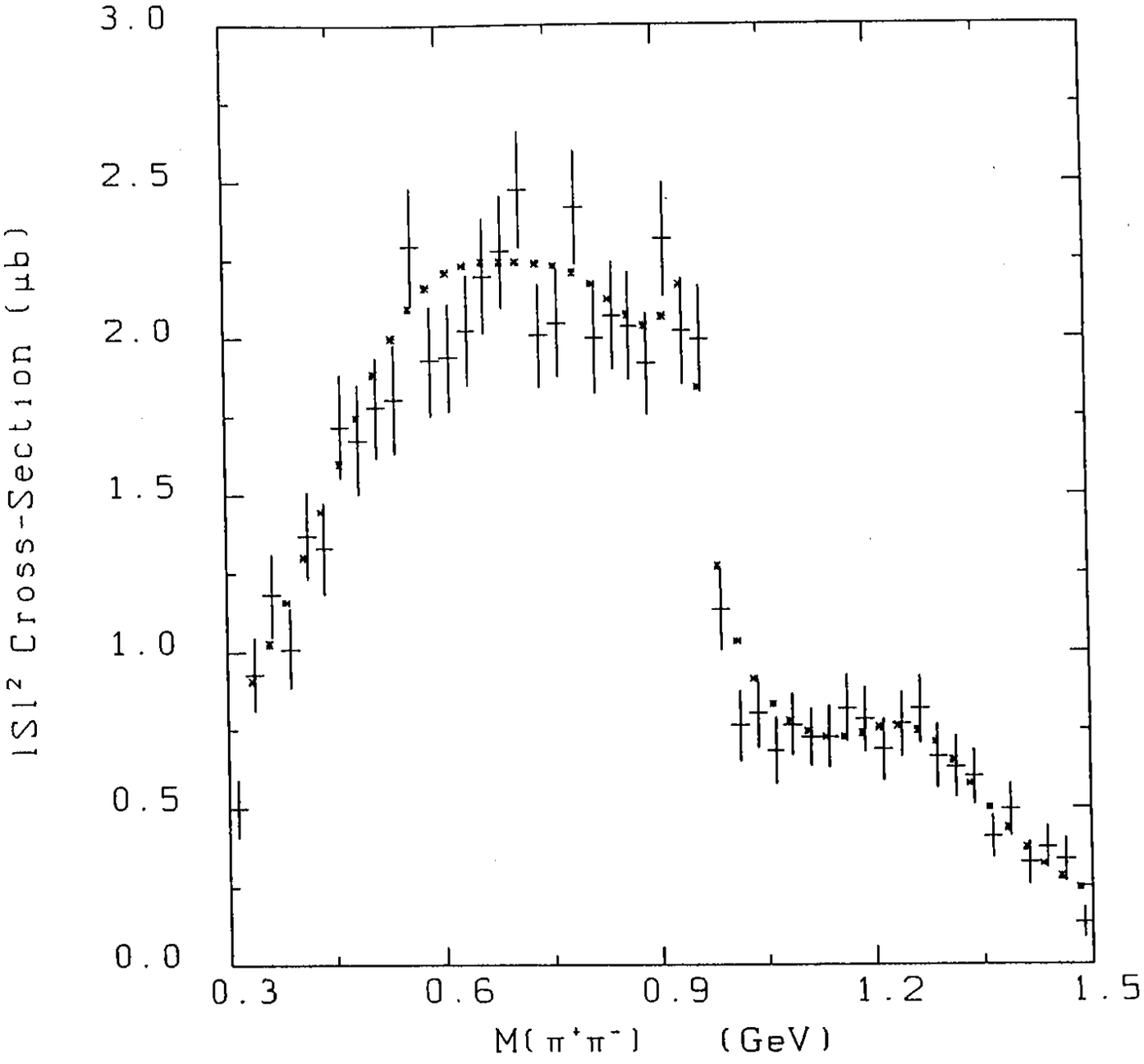

Fig.7

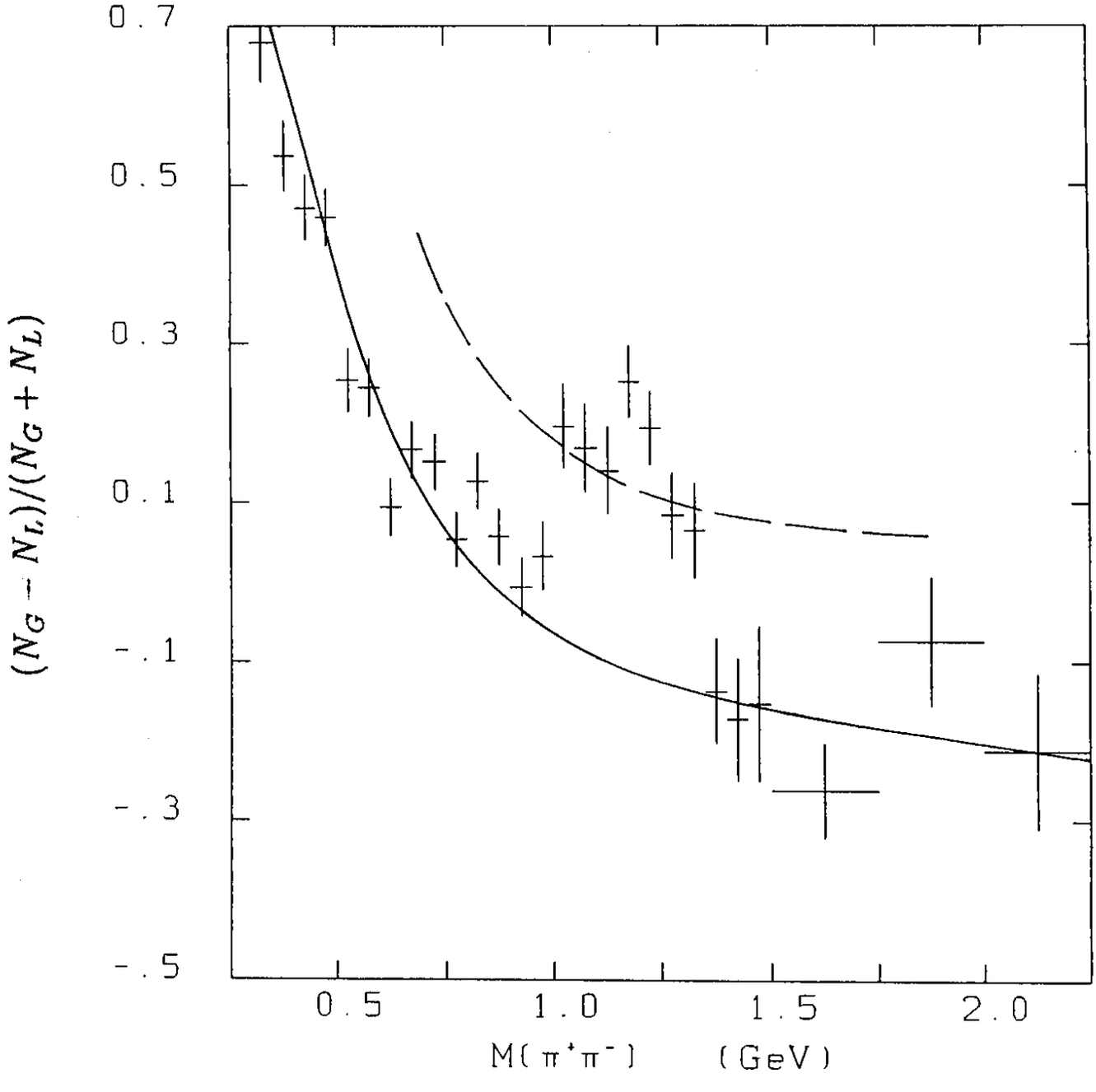

Fig.8

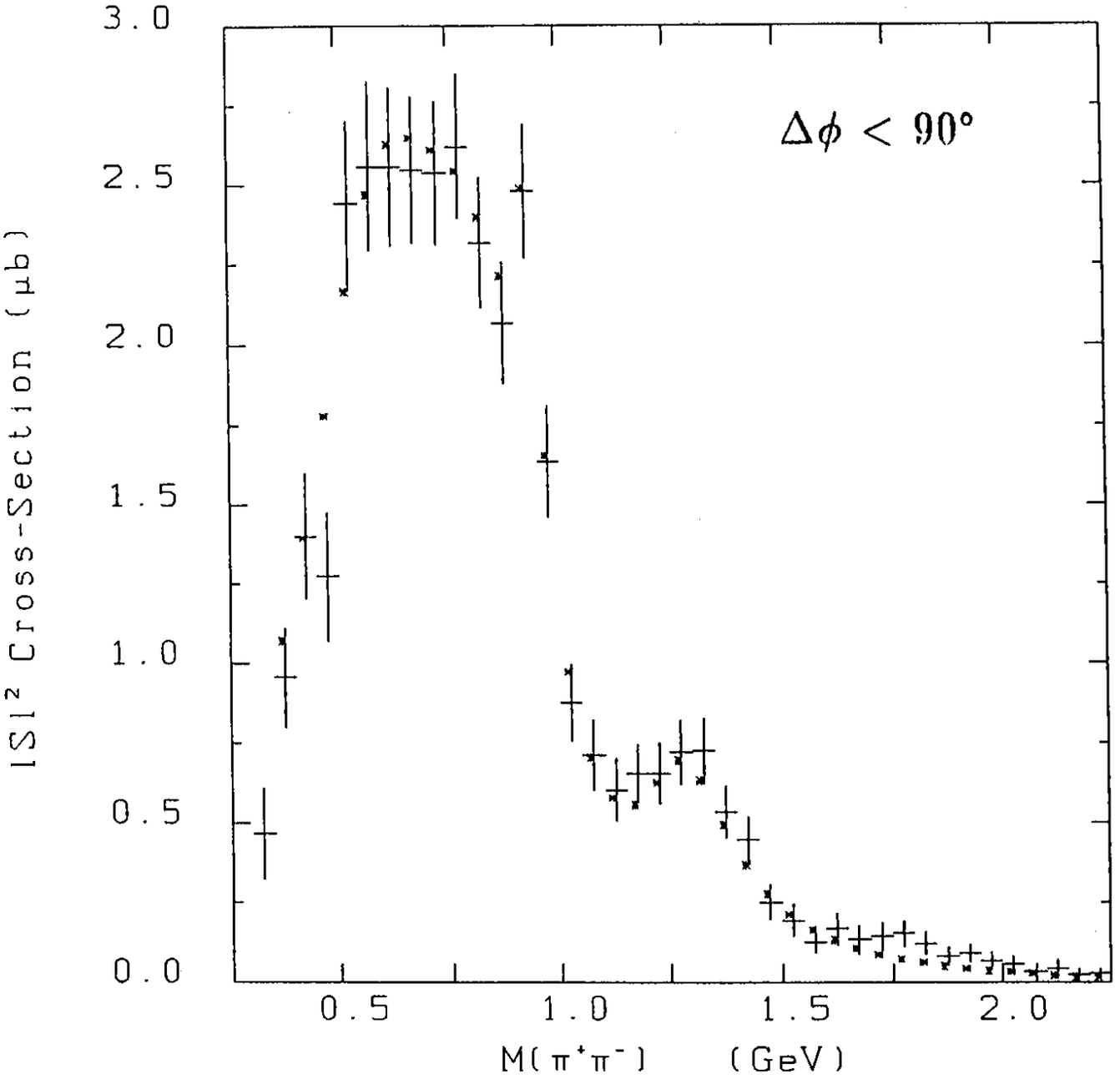
3.0
2.5
2.0
1.5
1.0
0.5
0.0
$|S|^2$ Cross-Section (μb)
$\Delta\phi < 90°$
0.5
1.0
1.5
2.0
M($\pi^+\pi^-$) (GeV)

Fig.9 (a)

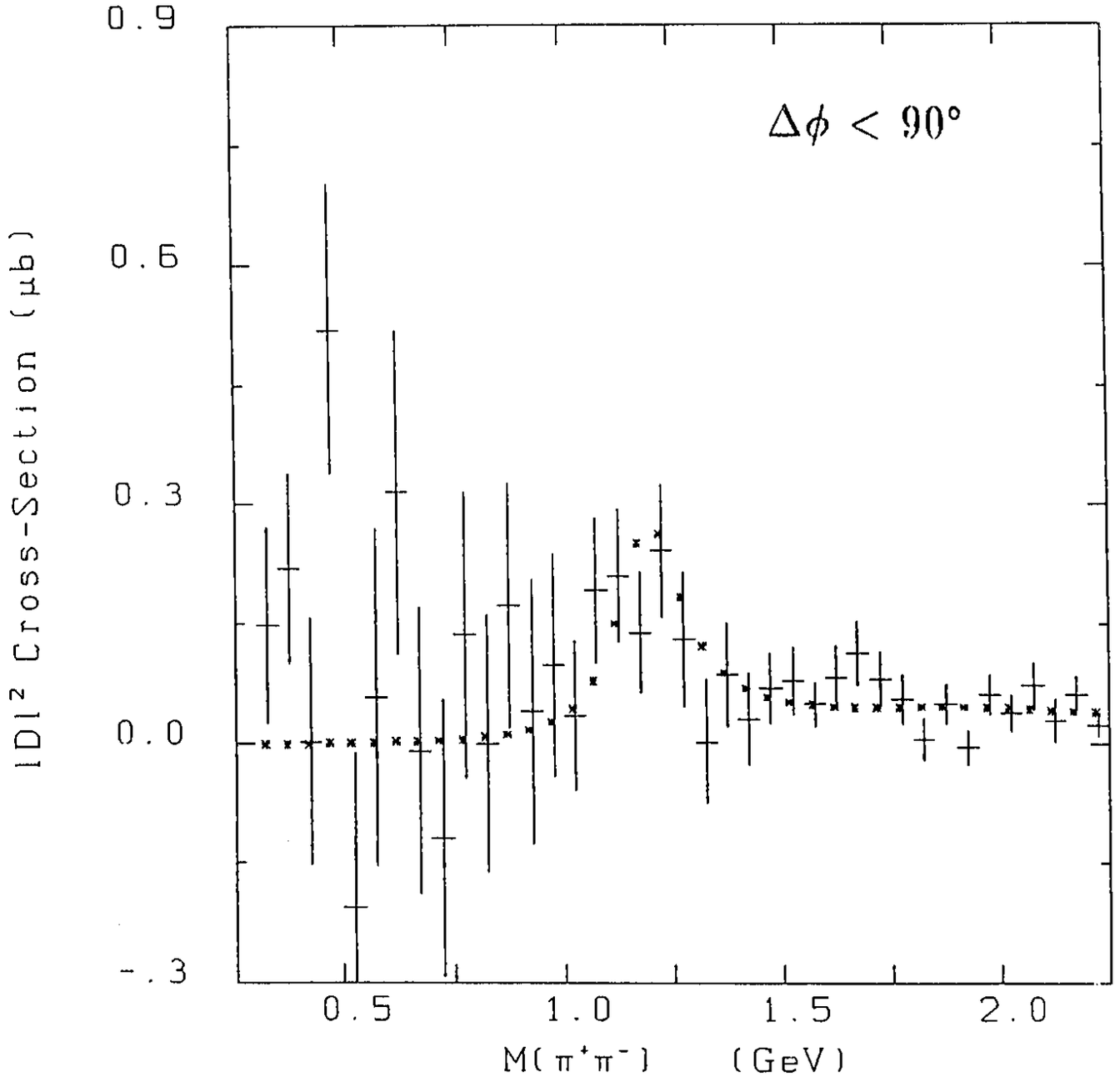

Fig.9 (b)

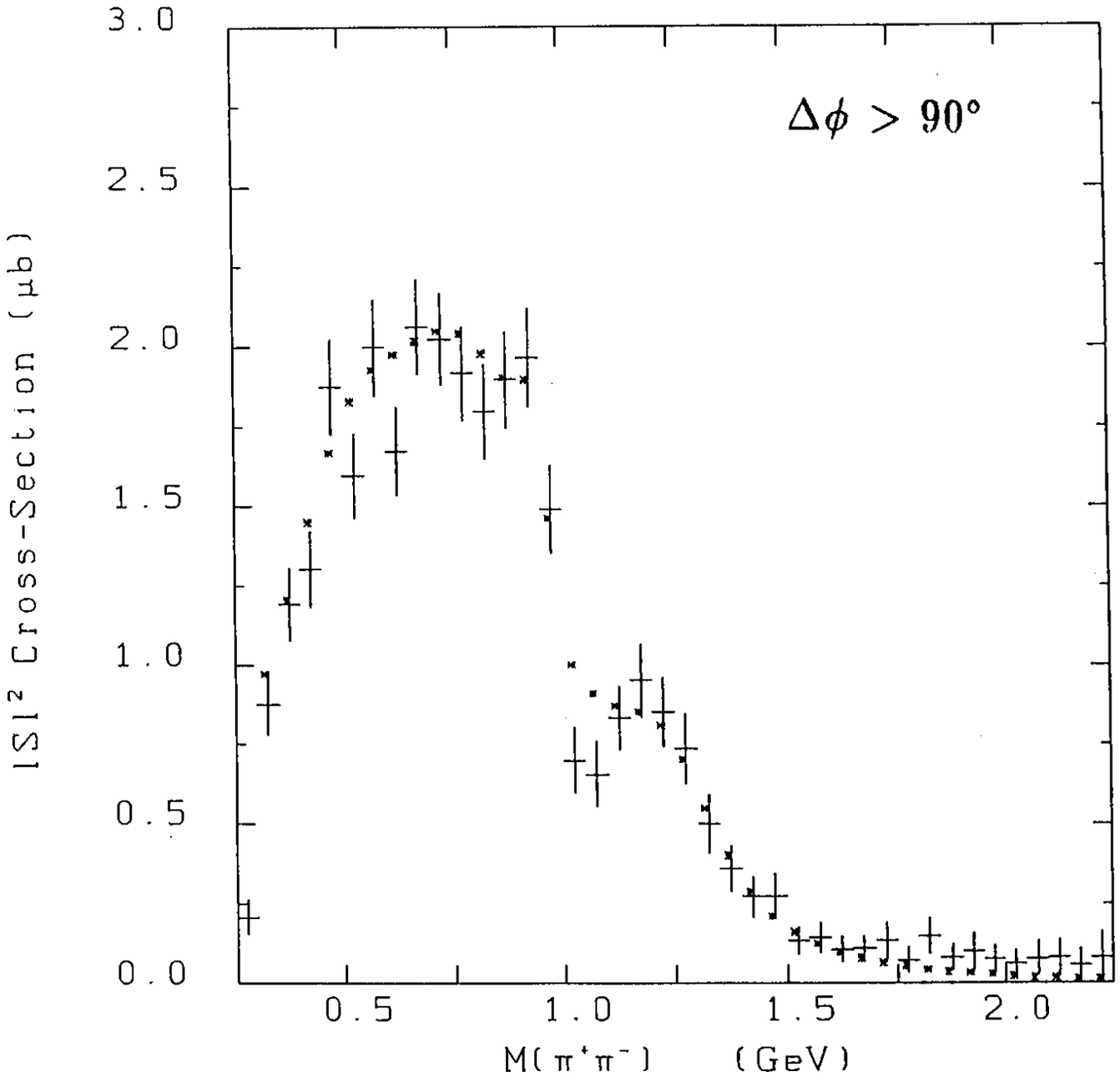
$\Delta\phi > 90°$
$|S|^2$ Cross-Section (μb)
M($\pi^+\pi^-$) (GeV)
3.0
2.5
2.0
1.5
1.0
0.5
0.0
0.5
1.0
1.5
2.0

Fig.10 (a)

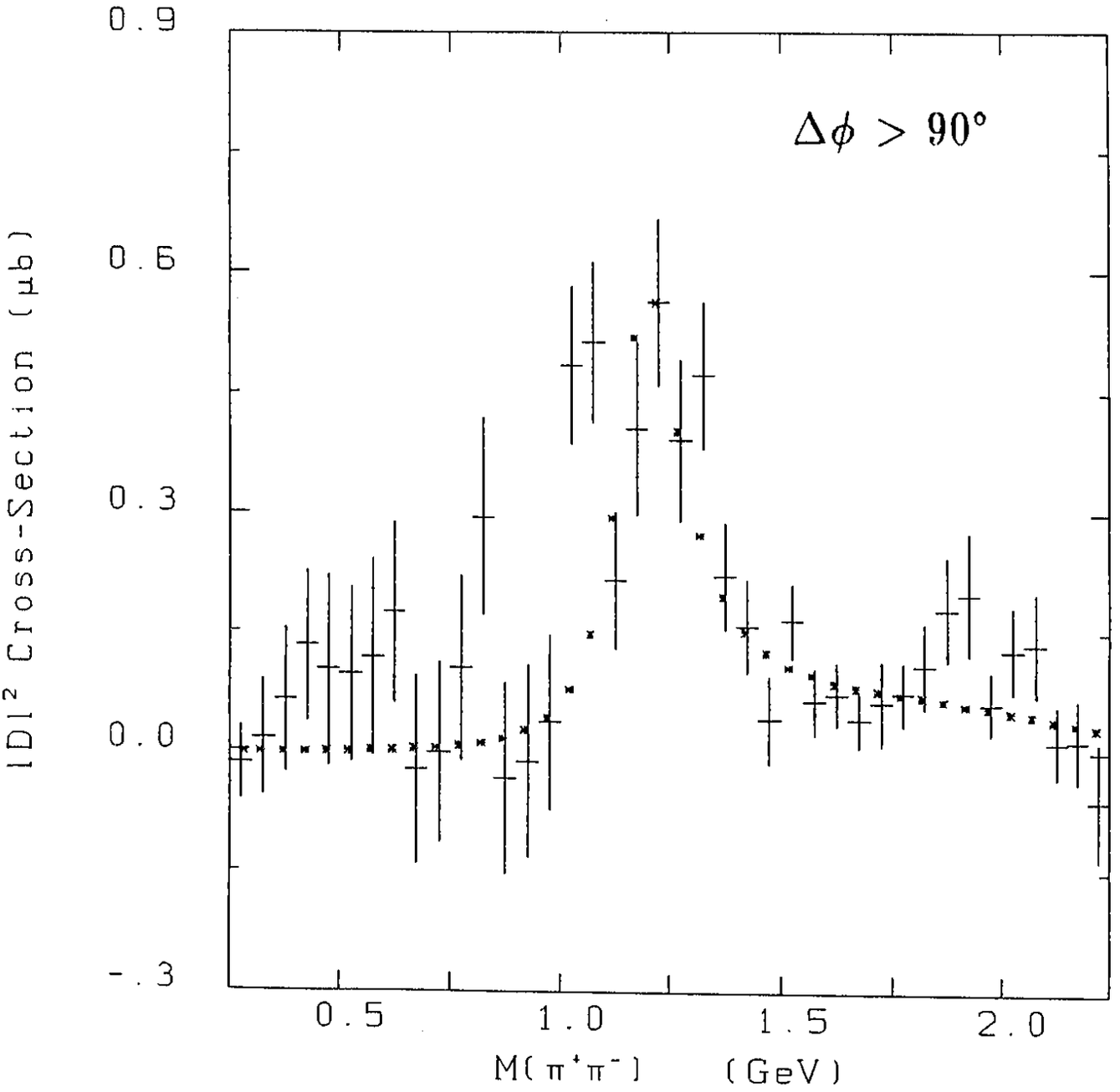
0.9
0.6
0.3
0.0
-.3
$|D|^2$ Cross-Section (μb)
$\Delta\phi > 90°$
0.5
1.0
1.5
2.0
M($\pi^+\pi^-$) (GeV)

Fig.10 (b)

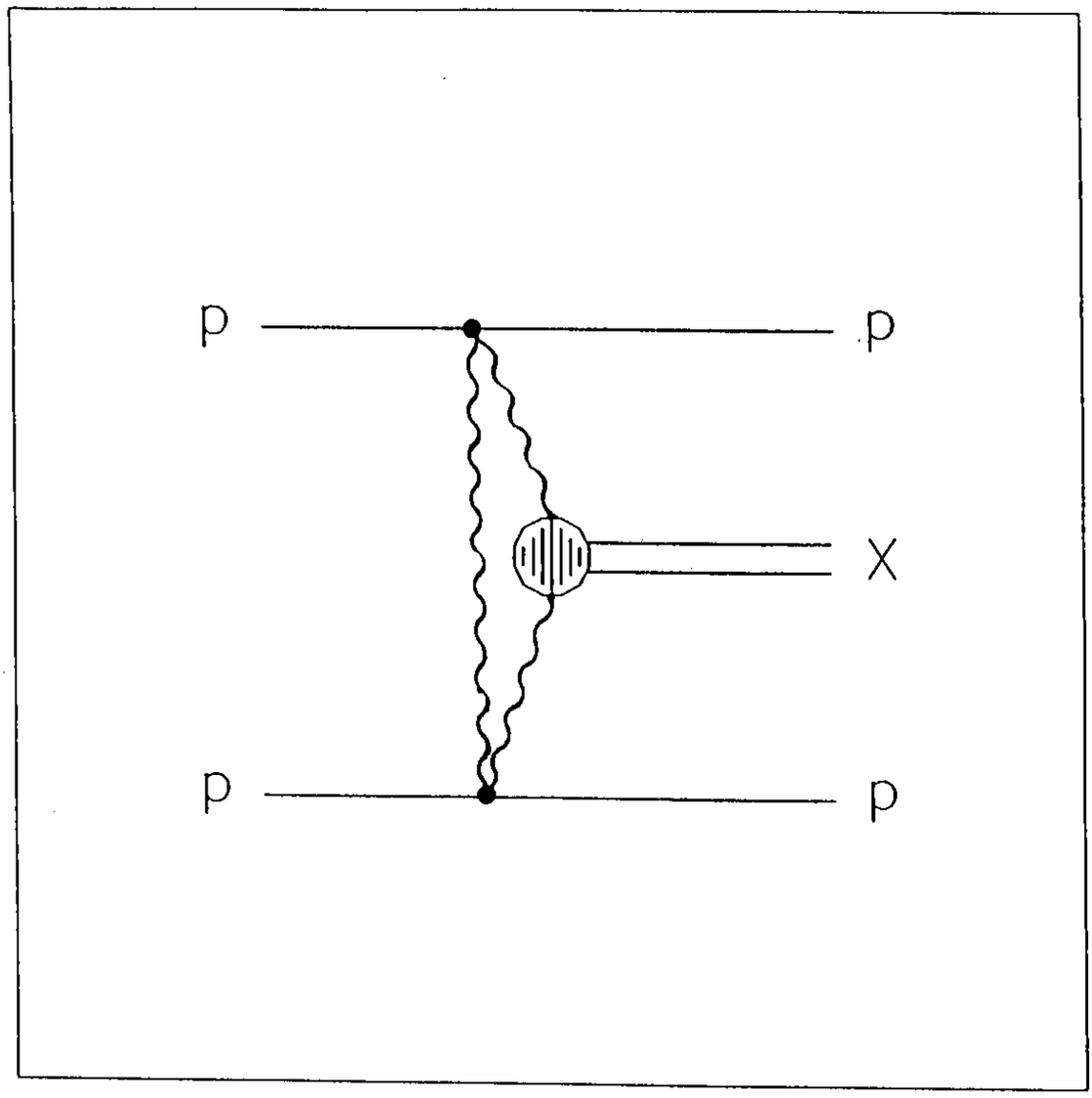

Fig.11